Available online at www.sciencedirect.com
ScienceDirect
Biochimica et Biophysica Acta 1768 (2007) 146–154
Biochimica et Biophysica Acta
BBA
www.elsevier.com/locate/bbamem

Preferential accumulation of Aβ(1−42) on gel phase domains of lipid bilayers: An AFM and fluorescence study

A. Choucair [a], M. Chakrapani [a,b], B. Chakravarthy [c], J. Katsaras [b,d], L.J. Johnston [a,*]

[a] *Steacie Institute for Molecular Sciences, National Research Council Canada, Ottawa, ON, Canada K1A 0R6*
[b] *Canadian Neutron Beam Centre, National Research Council Canada, Chalk River, ON, Canada K0J 1J0*
[c] *Institute for Biological Sciences, National Research Council Canada, Ottawa, ON, Canada K1A 0R6*
[d] *Biophysics Interdepartmental Group and Guelph-Waterloo Physics Institute, University of Guelph, Guelph, ON, Canada NIG 2W1*

Received 1 June 2006; received in revised form 7 September 2006; accepted 8 September 2006
Available online 20 September 2006

Abstract

Peptide–membrane interactions have been implicated in both the toxicity and aggregation of β-amyloid (Aβ) peptides. Recent studies have provided evidence for the involvement of liquid-ordered membrane domains known as lipid rafts in the formation and aggregation of Aβ. As a model, we have examined the interaction of Aβ(1−42) with phase separated DOPC/DPPC lipid bilayers using a combination of atomic force microscopy (AFM) and total internal reflection fluorescence microscopy (TIRF). AFM images show that addition of Aβ to preformed supported bilayers leads to accumulation of small peptide aggregates exclusively on the gel phase DPPC domains. Initial aggregates are observed approximately 90 min after peptide addition and increase in diameter to 45–150 nm within 24 h. TIRF studies with a mixture of Aβ and Aβ–Fl demonstrate that accumulation of the peptide on the gel phase domains occurs as early as 15 min after Aβ addition and is maintained for over 24 h. By contrast, Aβ is randomly distributed throughout both fluid and gel phases when the peptide is reconstituted into DOPC/DPPC vesicles prior to formation of a supported bilayer. The preferential accumulation of Aβ on DPPC domains suggests that rigid domains may act as platforms to concentrate peptide and enhance its aggregation and may be relevant to the postulated involvement of lipid rafts in modulating Aβ activity *in vivo*.
© 2006 Elsevier B.V. All rights reserved.

Keywords: β-amyloid peptide; Atomic force microscopy; Bilayer; Fluourescence

1. Introduction

Alzheimer's disease (AD) is a chronic neurological disease, leading to progressive mental degeneration and irreversible dementia. Pathologically, AD is characterized by the presence of neurofibrillary tangles and extracellular senile plaques in affected areas of the brain [1]. The main constituent of these plaques is β-amyloid (Aβ), a 39 to 43 amino acid peptide, produced intracellularly from the enzymatic cleavage of a transmembrane protein known as amyloid precursor protein (APP) [2]. Genetic data suggest that Aβ is involved in the pathogenesis of AD [3], and several *in vitro* studies show a clear correlation between the aggregation and fibrillation of Aβ, and its neurotoxicity [4,5]. Traditionally, insoluble plaques and fibrils of Aβ were believed to be responsible for the neurological degeneration observed in AD. However, more recent studies show that small diffusible nonfibrillar oligomers of Aβ [6–9] as well as intermediate species formed during Aβ fibrillation (protofibrils) [10] are also toxic to cultured neurons. It has been suggested that plaques may act as a reservoir of species in equilibrium with small neurotoxic oligomers [11]. Recently, it was reported that soluble oligomers of Aβ are responsible for memory deficits in middle aged rats occurring prior to tangles or plaque formation; these oligomers could also induce memory impairment when injected into young rats [12]. Despite the growing body of evidence that links Aβ to AD, the exact mechanism through which soluble monomers of Aβ aggregate *in vivo*, interact with cellular membranes and elicit a neurotoxic effect is still not clear [1].

Abbreviations: AD, Alzheimer's disease; Aβ, Amyloid β; APP, amyloid precursor protein; AFM, atomic force microscopy; DOPC, 1,2-dioleoyl-*sn*-glycero-3-phosphocholine; DPPC, 1,2-dipalmitoyl-*sn*-glycero-3-phosphocholine; TIRF, total internal reflection fluorescence; TR-DHPE, Texas Red® 1,2-dihexadecanoyl-*sn*-glycero-3-phosphoethanolamine, triethylammonium salt

* Corresponding author.
E-mail address: Linda.Johnston@nrc-cnrc.gc.ca (L.J. Johnston).

0005-2736/$ - see front matter © 2006 Elsevier B.V. All rights reserved.
doi:10.1016/j.bbamem.2006.09.005

Several hypotheses have been proposed to explain the toxic action of β-amyloid. Among these, non-specific interactions with lipid membranes have been implicated in both Aβ aggregation and toxicity [13]. For example, it was shown that membrane components such as cholesterol and gangliosides enhance the binding of Aβ to lipid bilayers, and act as seeds that promote the self-aggregation of the peptide [14–16]. It was also reported that the interaction of Aβ with negatively charged lipids or with gangliosides induces a change in the peptide secondary structure and promotes the formation of the β-sheet structure that is required for Aβ aggregation [17–20]. Other studies have demonstrated that the addition of Aβ to lipid vesicles compromises the membrane integrity, causing leakage of dye molecules encapsulated in the vesicle interior [19,21,22]. Aβ was also reported to form ion-channels in planar lipid bilayers and lipid vesicles, and to induce neurotoxicity by altering the ionic homoeostasis [23–27].

Most studies of the interaction of Aβ with model membranes have examined Aβ(1–40) which accounts for the largest fraction of secreted Aβ peptides. However, the more hydrophobic Aβ(1–42) is the predominant component in senile plaques [28] and displays enhanced neurotoxicity. Aβ(1–42) is an amphiphilic peptide, consisting of a polar N-terminal domain (residues 1–28) and a hydrophobic C-terminal (residues 29–42), and is more prone to aggregation than Aβ(1–40) [29,30]. Recent studies indicate that the two peptides oligomerize though distinct pathways [31] and there is conflicting evidence concerning the propensity of Aβ(1–42) to insert into and disrupt bilayer membranes. For instance, McLaurin et al. reported that Aβ(1–40) is more effective in inducing dye leakage from vesicles than Aβ(1–42) [19,21]. By contrast, other studies have shown that Aβ(1–42) forms channels and disrupts membranes [22,24].

Both Aβ and APP have been identified in lipid rafts isolated as detergent resistant membrane fractions from both cultured cells and brain [32–34]. Lipid rafts are microdomains that are rich in saturated lipids and cholesterol and that play an important role in aggregation of proteins for signal transduction and membrane trafficking [35,36]. Recent studies have shown that the cleavage of APP to produce Aβ peptides is regulated by the partitioning of APP and the β-secretase cleavage enzyme into lipid rafts [37] and that accumulation of dimeric Aβ and APP in lipid rafts may be linked to memory impairment [38]. The potential role of membrane domains in formation and aggregation of Aβ peptides has prompted us to examine the interaction of Aβ(1–42) with ordered lipid domains as a model for microdomains in cellular membranes. We have used a combination of atomic force microscopy (AFM) and fluorescence microscopy to probe the interaction of Aβ(1−42) with phase separated lipid bilayers prepared from DOPC/DPPC mixtures. Although several previous studies have used AFM to study the interaction of amyloid peptides with supported bilayers [20,24,39,40], this is the first example in which phase-separated membranes are examined. We have also used peptide concentrations that are below those required for aggregation in solution. The results demonstrate that addition of Aβ to preformed lipid bilayers leads to selective accumulation of the peptide on ordered gel phase domains, rather than the fluid phase, and eventually to formation of small spherical aggregates. By contrast, the peptide is distributed in both gel and fluid phases when it is incorporated in the lipid bilayer during vesicle formation. These results highlight the importance of membrane composition in controlling the behavior of Aβ, even for simple phosphatidylcholine mixtures in the absence of either cholesterol or charged lipids, and may have implications for the role of lipid rafts in modulating Aβ activity *in vivo*.

2. Materials and methods

2.1. Materials

1,2-Dioleoyl-*sn*-Glycero-3-Phosphocholine (DOPC) and 1,2-Dipalmitoyl-*sn*-Glycero-3-Phosphocholine (DPPC) were obtained from Avanti Polar Lipids (Alabaster, AL). Texas Red® 1,2-dihexadecanoyl-*sn*-glycero-3-phosphoethanolamine, triethylammonium salt (TR-DHPE) was obtained from Invitrogen Canada Inc. HPLC-grade chloroform (Fisher Scientific) and Milli-Q water, deionized to a resistivity of 18.5 MΩcm, were used in all of the experiments. β-Amyloid (1–42) peptide was purchased from Biopeptide Co., Inc. (San Diego, CA), and Fluorescein-β-Amyloid (1–42) (Fl–Aβ) from AnaSpec, Inc. (San Jose, CA). Both manufacturer's guarantee peptide purity >95% as determined by HPLC. The peptide was treated with 1 mM NaOH according to a literature procedure [41], lyophilized and stored at −80 °C. Before its addition to a lipid bilayer, the peptide was dissolved in 50 mM HEPES buffer (pH=7.8). Gel electrophoresis shows that the sodium hydroxide pretreatment gives predominantly monomeric Aβ, in agreement with literature results [41]. CD spectroscopy of freshly prepared solutions of ~60 μM Aβ shows minimal signal at 218 nm due to β-sheet; the signal due to β-sheet increases with time with a maximal yield obtained after 2 days incubation in solution at room temperature.

2.2. Vesicle preparation

Lipid stock solutions were prepared in chloroform and aliquots were mixed in a glass vial to give a DOPC:DPPC molar ratio of 1:1. In the case of Aβ-reconstituted vesicles, the peptide was mixed with the lipids to give a peptide to lipid molar ratio of 1:130. Chloroform was evaporated under a gentle stream of nitrogen gas, and the resulting lipid film was dried under vacuum overnight to remove trace amounts of solvent. The film was hydrated with Milli-Q water (final lipid concentration of 1 mg/ml) and vortexed for 2–3 min. The obtained turbid solution of multilamellar vesicles was then sonicated in a bath sonicator (Branson Instruments) at 38–42 °C to clarity (20–30 min).

2.3. Bilayer formation and AFM imaging

Supported lipid bilayers were prepared using the method of vesicle fusion. Briefly, to a piece of freshly cleaved mica clamped to the AFM liquid cell (Molecular Imaging), 300 μl of $CaCl_2$ (50 mM) and 150 μl of vesicle solution were added. The solution was incubated at room temperature for 30 min, which proved to be a sufficient time for the vesicles to fuse and rupture to form a uniform bilayer on mica. Prior to imaging, the bilayer was rinsed extensively with Milli-Q water to remove excess lipids and $CaCl_2$.

AFM measurements for all bilayers were carried out on a Mac mode PicoSPM atomic force microscope (Molecular Imaging Inc.) in aqueous solution. Magnetic coated silicon tips (Mac Lever type II) with a force constant=2.8 N/m and a resonance frequency in water between 20 and 25 kHz were used for wet imaging. The scan rate was kept at 1 Hz or less. After imaging the lipid bilayer, 10 μg of Aβ(1–42) were added to the AFM cell (final peptide concentration ≈ 3 μM) and the sample was incubated at room temperature. The bilayer was subsequently imaged at various time points. Several bilayers were prepared independently and incubated with Aβ. For each sample, several areas were scanned.

2.4. Peptide aggregation in solution and AFM imaging

Aβ(1–42) or a mixture of unlabeled and Fl–Aβ (10% w/w) were incubated in HEPES buffer (50 mM; pH=7.8) at 37 °C in a temperature controlled water

bath. The peptide concentration was 1 mg/ml. After ca. 24 h of incubation, 10 μl of the sample were placed on freshly cleaved mica, allowed to adsorb for about 5 min and then washed three times with 50 μl of water. The sample was subsequently dried with a gentle stream of nitrogen. AFM images of the peptide were obtained using a Multimode Nanoscope III (Digital Instruments, Santa Barbara, CA) operated in tapping mode. Ultrasharp noncontact rectangular silicon cantilevers with a spring constant of 40 N/m (MikroMasch, Wilsonville, OR) were used with a scan rate of 1 Hz. Height and sizes of aggregates were determined using the Nanoscope 5.12 program.

2.5. Total internal reflection fluorescence (TIRF) microscopy

Lipid bilayers were prepared on mica from a lipid mixture of DOPC:DPPC: TR-DHPE (TR-DHPE content = 0.5% mol/mol) as described above. A mixture of fluorescein-labeled and unlabeled peptide was added to the bilayer (15% w/w of Fl–Aβ) to give a final peptide concentration of ≈3 μM. All images were collected using an Olympus IX2-RFAEVA 2 inverted microscope (Olympus Corporation, Japan), equipped with a 488 nm Argon laser, a 543 nm He-Ne-G laser and a 60 X TIRF oil immersion objective. The collected fluorescence signal was detected using a CoolSnap ES CCD camera (Photometrics, Tucson, AZ). Images were analysed using Image-Pro 5.1 software.

2.6. Fluorescence anisotropy measurements

Steady state fluorescence anisotropy measurements were performed using a PTI fluorimeter equipped with xenon flash lamp and manual polarizers (Photon Technologies International, South Brunswick, NJ). Excitation and emission wavelengths were set at 360 and 427 nm, respectively. DOPC/DPPC vesicles, prepared as described above, were diluted to a final lipid concentration of 250 μg/ml and incubated for 1 hr with 1,6-diphenyl-1,3,5-hexatriene (DPH, Molecular Probes) at 1:500 probe: lipid molar ratio. The fluorescence anisotropy of the solution was measured at room temperature before and after the addition of Aβ to the vesicle solution (incubation for 1 hr; final peptide concentration 4 μM).

Fluorescence anisotropy was calculated as:

$$r = \frac{I_{VV} - gI_{VH}}{I_{VV} + 2gI_{VH}}$$

where I_{VV} and I_{VH} are the fluorescence intensity when the excitation and emission polarizers are parallel and perpendicular, respectively. The g-factor was calculated by exciting with horizontally polarized light and collecting vertically, $I_{HV,}$ and horizontally, I_{HH}, polarized emission:

$$g = \frac{I_{HV}}{I_{HH}}$$

3. Results

3.1. Phase separated DOPC/DPPC bilayers

AFM images of DOPC/DPPC (1:1 molar ratio) bilayers in water show a phase separated membrane with higher gel phase DPPC domains in a range of sizes and shapes surrounded by a fluid DOPC phase (Fig. 1). This is consistent with an earlier AFM study for this mixture [42] and with the phase transition temperatures for DOPC and DPPC (−18 °C, and 40 °C, respectively). As shown in Fig. 1A, bilayers imaged approximately 1 h after preparation typically showed domains with two distinct heights; the higher domains extend ca. 1.2±0.1 nm (n=22) above the fluid phase and range in size between 200 and 800 nm. The lower domains are ca. 0.8±0.1 nm (n=16) higher than the fluid phase and are located either on the edges of the higher domains, or as isolated domains that range in size from 140 to 400 nm. The relative surface area covered by each type of domain varied from sample to sample and also changed with time. For instance, the bilayer shown in Fig. 1A was imaged 1 day after preparation (Fig. 1B) and showed only larger domains with a uniform height (1.3±0.2 nm (n=16)). Fig. 1C shows an image of a freshly prepared bilayer that has predominantly the higher domains (domain height = 1.4±0.3 nm; n=25). Such bilayers did not change significantly over a period of 48 h (data not shown).

The presence of domains with two distinct heights is attributed to a compositional asymmetry in the upper and lower leaflets of the bilayers. The higher domains correspond to areas in the membrane where DPPC molecules overlap in both leaflets, while the shorter domains result from the asymmetric transmembrane distribution of lipids (DOPC on DPPC, or vice versa). The formation of domains with two different heights was reported for phase separated lipid bilayers of DOPC/SM [43] and DSPC/DLPC [44] and was explained by an asymmetric distribution of lipids in the bilayer leaflets. By contrast, in a previous study of DOPC/DPPC domains with a uniform height of 1.21±0.03 nm were reported and were assigned to areas with gel phase DPPC completely superimposed in the two leaflets [42]. We attribute this domain symmetry to the higher temperature used (60 °C) for both vesicle sonication and bilayer formation [42]. This is consistent with the results of Lin et al. which showed that the formation of symmetric domains in DSPC/DLPC bilayers depended on the thermal history of the sample [44] and with our observation that increases in sonication temperature and time favor the formation of symmetric domains in DOPC/DPPC bilayers.

3.2. AFM studies of the interaction of Aβ with DOPC/DPPC bilayers

DOPC/DPPC bilayers were incubated with freshly prepared solutions of 3 μM Aβ(1–42) at room temperature. The peptide–bilayer interaction was followed by imaging the bilayer in aqueous solution after 60, 85, 90, 100 and 125 min of incubation as shown for selected time points in Fig. 2. Small aggregates of Aβ started to accumulate on the domains after approximately 85–90 min (Fig. 2B), with an average height of ca. 1.5±0.8 nm and a diameter ranging between 36 and 58 nm (average diameter = 45±7 nm). The height and diameter of the aggregates increased with incubation time, and after approximately 125 min, the aggregates extend ca. 2.4±0.7 nm above the fluid phase, and have an average diameter of 69±8 nm. After 19 h, the extent of peptide accumulation increased, and aggregates were observed uniformly distributed on the gel phase of the bilayer (DPPC-rich domains) but were not detected in the fluid phase. The aggregates extend *ca.* 4±1 nm (n=24) above the fluid phase and are approximately 70–150 nm in diameter (Fig. 2C). For comparison, a control bilayer of DOPC/DPPC was prepared and imaged after 1 and 24 h (data not shown). The domains in the control bilayer show no evidence for the small aggregates observed for the peptide-incubated bilayers. Note that the images at later time points which have significant Aβ accumulation on the gel phase domains (Fig. 2C, D) do not show sharp well-resolved peptide aggregates. This

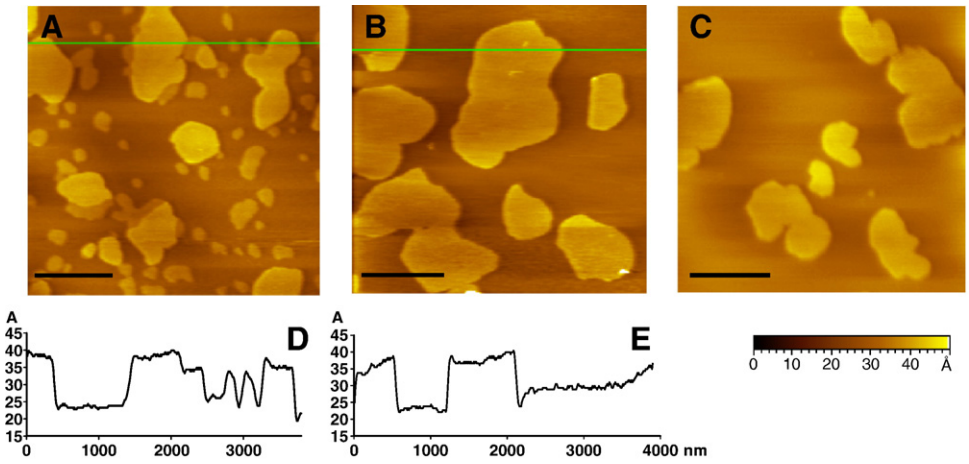

Fig. 1. AFM images of 1:1 DOPC/DPPC bilayers showing a bilayer immediately (A) and 1 day after preparation (B) and a second bilayer immediately after preparation (C). Scale bars are 1 μm and all images were obtained in water. Cross sections (height vs. surface distance) for the lines marked in images A and B are shown in panels D and E, respectively.

indicates that the peptide aggregates are only weakly attached to the membrane and thus are very easily moved by the tip, leading to slightly fuzzy, streaky features.

For bilayers with both symmetric and asymmetric domains, Aβ aggregates are observed exclusively on the higher domains which contain DPPC in both leaflets. The accumulation on the high domains, as opposed to the fluid phase or the lower domains was maintained even after 48 h of incubation (Fig. 2D). The absence of peptide aggregates on asymmetrical domains suggests that these domains have DOPC in the upper leaflet and DPPC in the leaflet proximal to the solid support, and not vice versa.

Bilayers incubated with Aβ(1–42) for longer than 1 day frequently developed a number of bilayer defects. However, the extent of damage was not significantly larger than that observed in control bilayers that were stored in water for a similar length of time. Bilayers with significant membrane damage also had large lipid aggregates which are not readily distinguished from peptide, making it impractical to image bilayers for longer periods of time. We obtained no evidence for fibril formation for any of the incubation conditions (up to 2 days at room temperature).

Several experiments were carried out in order to help distinguish between peptide aggregation in solution and on the membrane. Note that the peptide concentration used for the bilayer incubations is well below the typical threshold concentration (10–20 μM) required for fibril or oligomer formation in solution [45,46]. To confirm that the peptide samples used aggregate to form the expected fibrils in solution at high concentrations, we incubated Aβ samples at 1 mg/ml at 37 °C and observed significant yields of fibrils within 1 day (Fig. 3A). By contrast, aliquots of freshly prepared 3 μM Aβ (as used for bilayer experiments) imaged on mica showed only small globular aggregates that were approximately 1.3 nm in height with an apparent diameter of 20–30 nm. Heights of ~1 nm are typically assigned to either monomers or small oligomers of Aβ. Note that the apparent diameter is largely determined by the size of the AFM tip and is less useful for assessing the extent of oligomerization [45]. These experiments, in combination with the fluorescence results described

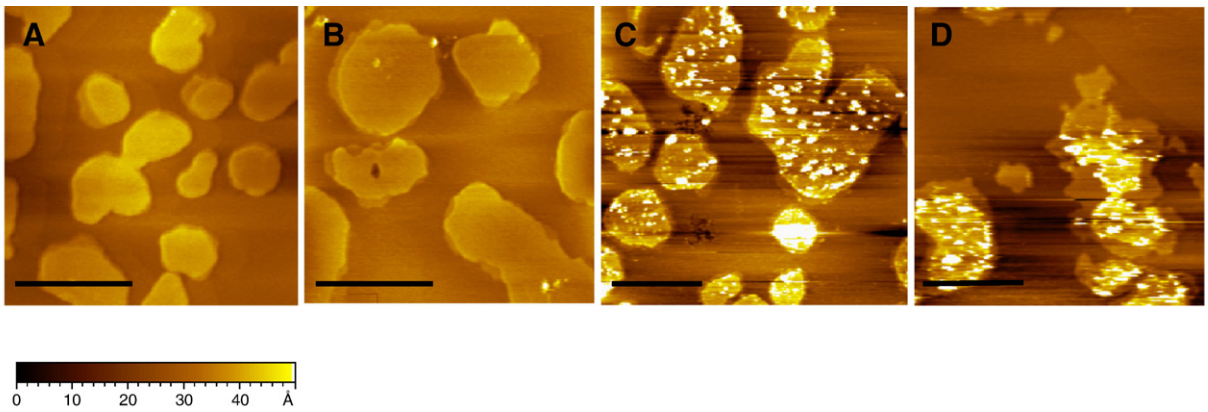

Fig. 2. AFM images of a 1:1 DOPC/DPPC bilayer before (A) and after incubation with 3 μM Aβ(1–42) for (B) 90 min and (C) 19 h. Image D shows a second bilayer after 48 h of incubation; in this case asymmetric domains are observed. Scale bars are 1 μm and all images were obtained in water.

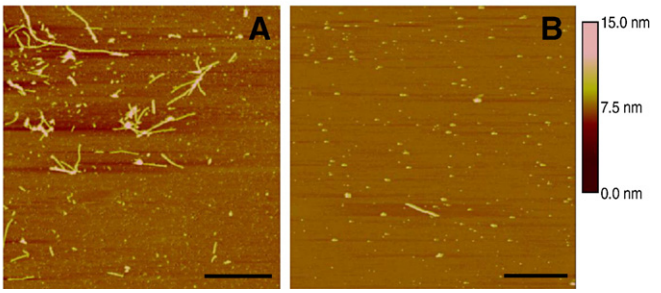

Fig. 3. AFM images for peptide samples (dry, mica) after incubation of 1 mg/ml solutions of Aβ (A) and Aβ/Fl–Aβ (9:1, B) at 37 °C for 24 h. Scale bars are 1 μm for all images.

below, indicate that aggregation of the peptide does not occur in solution.

3.3. TIRF microscopy studies of Aβ-bilayer interactions

Fluorescence microscopy was used to examine the interaction of Aβ with supported bilayers in order to provide more information about peptide–membrane interactions at early times prior to the observation of peptide aggregates by AFM. In these experiments 1:1 DOPC/DPPC vesicles were prepared with 0.5% Texas Red-DHPE, which is known to partition preferentially into fluid membrane phases [47]. Lipid bilayers were prepared on mica as described above and imaged using a total internal reflection fluorescence microscope. TIRF is an interface sensitive method that probes fluorescence within ~100 nm of the surface and therefore readily detects peptide bound to the membrane with no background signal due to residual labeled peptide in solution. Fig. 4A shows the fluorescence image of a phase separated bilayer of DOPC/DPPC/TR-DHPE after excitation with the 543 nm laser. The dark areas correspond to DPPC gel phase domains from which the fluorescent lipid is completely excluded. The domain size ranges between 300 and 700 nm, consistent with that determined from AFM images.

To follow the early stages of peptide–membrane interactions, an aqueous solution of fluorescein-labeled and unlabeled Aβ (3 μM, 85/15 Aβ/Fl–Aβ) was added to the bilayer in the liquid cell. Excitation of the bilayer at 488 nm resulted in the appearance of small fluorescent domains, indicating accumulation of peptide on the bilayer. These bright domains were detected as early as 8 min after peptide addition and were clearly visible after 15 min. Shown in Fig. 4B, C are sequential 488 and 543 nm TIRF images of the bilayer 30 min after the addition of the peptide. Comparison of Fl and Texas Red excitation showed that the bright fluorescent domains due to the peptide corresponded to the dark domains from which the Texas Red-DHPE was excluded. The preferential accumulation of the peptide on the gel phase was maintained even after 1 day of incubation (consistent with AFM results for the unlabeled peptide). Fig. 4D, E show 488 and 543 nm images of the bilayer after 19 h of incubation with the peptide, indicating little change in the intensity of the fluorescent domains over this time period. For comparison an overlay of the two images demonstrating the selective accumulation of peptide on the gel phase domains is also shown (Fig. 4F). Note that there are a few larger domains in these images as compared to images of the same bilayer at early times, indicating some coalescence of smaller domains.

Although the accumulation of the peptide on the bilayer was clearly detected using TIRF as early as 8 min after incubation, AFM images of DOPC:DPPC:TR-DHPE bilayers incubated with a mixture of Aβ and Fl–Aβ (85/15 w/w) reveal a low level of peptide accumulation on the bilayer, even after 19 h of

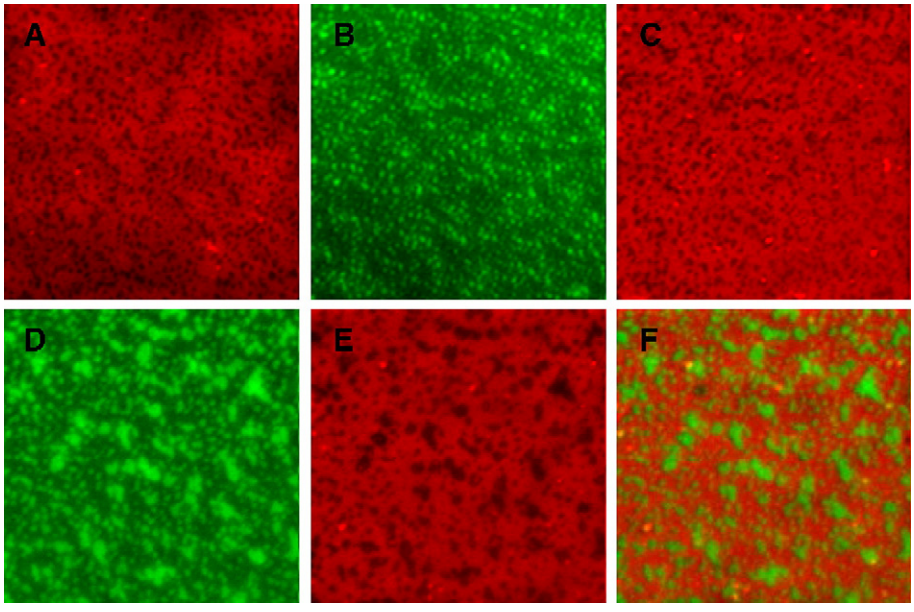

Fig. 4. TIRF images of a 1:1 DOPC/DPPC bilayer with 0.5% Texas Red-DHPE before (A, 488 nm excitation) and after incubation with 3 μM Aβ/Fl–Aβ (85/5) for 30 min (B, 488 nm in green, C, 543 nm in red) and 19 h (D, 488 nm in green, E, 543 nm in red; F, overlay of Fl and Texas Red). All images are 25 × 25 μm^2 and were obtained in aqueous solution. (For interpretation of the references to colour in this figure legend, the reader is referred to the web version of this article.)

incubation (data not shown). It is likely that the addition of the fluorescein label disrupts the aggregation of the peptide and prevents the formation of large aggregates that can be resolved with AFM. In fact, results of solution incubations of a mixture of fluorescein-labeled (10% Fl–Aβ) and unlabeled Aβ(1–42) show that the dye interferes with and delays the aggregation of the peptide. For instance, after 24 h of incubating unlabeled Aβ at 37 °C (conc.=1 mg/ml), AFM images reveal the formation of long and medium length fibrils (Fig. 3A). However, AFM images of the mixture of labeled and unlabeled peptide, incubated under the same conditions, indicate that fewer and shorter fibrils are formed (Fig. 3B). A previous study of Aβ aggregation showed that 0.1 μM NBD-labeled Aβ(1–40) did not interfere significantly with peptide aggregation for 1–50 μM total peptide concentration [48]. Either the lower levels of labeled peptide, the fact that the dye was attached via 2 additional "spacer" amino acids or differences between Aβ(1–40) and Aβ(1–42) could account for the much slower aggregation that we observe with Fl–Aβ.

3.4. Reconstitution of Aβ in DOPC/DPPC vesicles

The AFM and TIRF experiments both provide clear evidence for selective interaction of Aβ with gel phase DPPC domains. In order to test for any preference for gel vs. fluid phases for samples in which the peptide was directly incorporated in the bilayer, we reconstituted Aβ in DOPC/DPPC vesicles for preparation of supported bilayers. AFM images of such bilayers showed aggregates of Aβ(1–42) randomly distributed in both the fluid and gel phases (Fig. 5). Aggregates in the fluid phase are ca. 0.9±0.3 nm in height. Those present on the domains extend approximately 1.4±0.3 nm above the fluid phase. The aggregate diameter ranges between 30 and 100 nm, with an average of 60±16 nm and neither the heights or diameters increase over a period of several hours. The height of the aggregates is in good agreement with earlier studies by Lal for Aβ reconstituted in DOPC bilayers [24]. In this work high resolution AFM images indicated formation of Aβ channels comprised of tetrameric and hexameric peptide aggregates that extended approximately 1 nm above the fluid DOPC bilayer with diameters between 8 and 12 nm. At the level of resolution shown in Fig. 5 it is not possible to determine whether the larger aggregates that we detect correspond to clusters of oligomeric channels or some other type of aggregate. However, it is useful to note that the heights of the reconstituted peptide are significantly less than those observed for Aβ aggregates produced after several hours of incubation with preformed DOPC/DPPC bilayers.

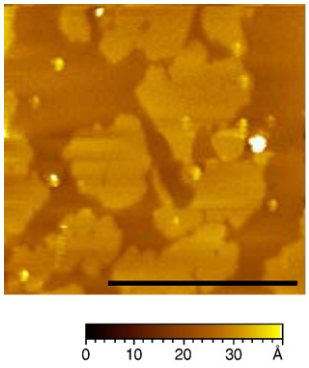

Fig. 5. AFM image of a 1:1 DOPC/DPPC bilayer with reconstituted Aβ (1:130 peptide/lipid ratio, scale bar of 1 μm, imaged in water). The bilayer was imaged ~1 h after preparation and does not change with time over a period of several hours.

3.5. Fluorescence anisotropy studies

Fluorescence anisotropy measurements with DPH were used to probe for possible peptide insertion in the membrane when Aβ is incubated with preformed vesicles. DPH is sensitive to changes in the lipid acyl chain ordering and has been used in a number of earlier studies to aid in distinguishing between inserted and surface adsorbed peptide [49–51]. The ratio of DPH probe concentration in fluid and gel phases has been shown to be independent of either probe concentration of relative amounts of the two lipid phases [52]. Measured anisotropies of 0.18±0.01 were obtained for DPH in DOPC/DPPC vesicles alone, and incubating the vesicles with 3.6 μM Aβ for 1 h did not result in any detectable change in anisotropy. By contrast, reconstituting the peptide into vesicles at peptide: lipid ratio of 1:25 resulted in a significant increase in anisotropy to 0.27±0.01, consistent with earlier studies which showed that peptide insertion leads to a decrease in membrane fluidity. Thus, we conclude that addition of Aβ(1–42) to preformed DOPC/DPPC vesicles does not lead to significant insertion of peptide into the acyl chain region of the bilayer.

4. Discussion

Both AFM and TIRF results clearly demonstrate that Aβ interacts preferentially with the ordered gel phase domains of phase separated DPPC/DOPC bilayers. The two techniques provide complementary data with fluorescence being particularly useful to follow the association of Aβ with the bilayer at early times before aggregates are detectable using AFM. The accumulation of the unlabeled peptide on the membrane leads to formation of small aggregates that can be detected after approximately an hour and which continue to increase in size. After approximately 1 day the aggregates have heights of 1–3 nm, similar to the height of oligomers formed in solution incubations at higher peptide concentrations [45,46]. There are several pieces of evidence that suggest that the aggregation of the peptide is facilitated by the membrane. Firstly, TIRF imaging shows that the peptide accumulates on the gel phase domains within a few minutes of adding Aβ to the bilayer, with the gel phase domains showing a constant fluorescence intensity after approximately 15 min. By contrast, peptide aggregates are only detected after more than 1 h and continue to grow in size over many hours. This result, plus the observation that concentrations considerably higher than 3 μM are required to promote Aβ oligomerization in solution (both from our studies and the literature), are consistent with membrane adsorption of peptide, followed by membrane facilitated aggregation. An

earlier study showed that adsorption of Aβ to a DMPC monolayer promoted the formation of β-sheet structures that were not present in aqueous solution [53]. Both the high local concentration at the membrane surface and the formation of β-sheet structures will facilitate aggregation on the gel phase domains. We do not find any evidence for fibril formation or bilayer damage, beyond that observed for control bilayers stored for similar time in the absence of peptide.

The accumulation of Aβ on gel phase domains of DPPC/DOPC bilayers does not appear to lead to insertion in the membrane. This is supported by the following two experiments. First, the fluorescence anisotropy results show clear differences between direct incorporation of Aβ in lipid mixtures prior to vesicle formation and the addition of Aβ to preformed vesicle bilayer membranes. These differences are consistent with peptide association with preformed bilayers leading to primarily surface adsorption. Second, AFM images show very different morphologies for Aβ reconstituted in bilayers as compared to samples where peptide is incubated with preformed bilayers. The lack of insertion of Aβ is in agreement with a previous study that demonstrated that Aβ(1–42) adsorbs to the surface of a DMPC monolayer but does not insert significantly or otherwise perturb the membrane structure [53]. Furthermore, studies of dye leakage from vesicles have indicated that 1 μM Aβ(1–42) has minimal insertion in lipid vesicles [21,40]. It was postulated that the repulsive forces between the hydrophilic lipid head groups and the hydrophobic C-terminus of Aβ (1–42) prevent the insertion of the peptide into the bilayer and favor surface binding [40]. However, the lack of insertion is in contrast to a recent study which reported that 7.5 μM Aβ(1–42) causes significant dye leakage from POPC and POPC/sphingomyelin/cholesterol giant vesicles [22]. This apparent discrepancy may be due to the different peptide concentrations used.

Several previous studies have examined the interaction of Aβ(1–42) and Aβ(1–40) with supported lipid bilayers using AFM. Yip and McLaurin showed that incubation of Aβ(1–42) with supported bilayers of total brain lipid extracts resulted in the formation of small peptide aggregates that were randomly distributed across the bilayer [40]. After incubation for 12 h, these aggregates were 5–12 nm in height and 5–26 nm in width. Although the uniform bilayers obtained from the total brain extract mixture provide no information on the preference of the peptide for ordered versus fluid phases, it was reported that a higher cholesterol content in the bilayer led to increased membrane rigidity (as assessed by DPH anisotropy) and a concomitant increase in accumulation of Aβ(1–42). The enhanced peptide accumulation on more rigid bilayers is consistent with our observations of preferential accumulation of peptide on ordered gel phase domains. The same study found that Aβ addition induced a phase transition to generate an interdigitated lipid phase.

By contrast to the above observations, an AFM study of the interaction of Aβ(1–40) with supported bilayers of total brain lipids indicated that small aggregates formed at early times whereas fibrils started to appear after several hours [20]. Fibril formation destabilized the bilayer and resulted in the appearance of large lipid patches as well as defects in the membrane. In the case of DMPC bilayers, small aggregates of Aβ, 1.2 to 1.5 nm in height, were observed on the membrane. Although, the aggregates increased in size and height with time and induced damage to small areas of the bilayer, fibrils were not observed, even after 24 h of incubation. Similarly, Green et al. examined the interaction of Aβ(1–40) with POPC/POPG bilayers using AFM [39]. Small peptide aggregates appeared within 1–2 h and increased in size with time. After incubation overnight, AFM images revealed the formation of small defects (damage) on the bilayer. This study observed much more rapid deterioration of POPC/POPG bilayers upon exposure to human amylin peptide. Thus it is clear that the peptide structure, concentration and incubation time all determine the aggregation behavior and extent of membrane damage.

The accumulation and aggregation of Aβ on the symmetrical gel phase DPPC domains, rather than the fluid phase or the asymmetrical lower domains, was detected using both AFM and TIRF and was maintained even after 48 h of incubation. Since DOPC and DPPC have identical head groups, the observed selectivity is probably the result of a preference for the more ordered parts of the membrane, rather than any specific interaction between the lipid head group and the peptide. The orientation, packing and degree of hydration of the phosphatidylcholine head groups are all different for fluid and gel phase membranes and presumably some combination of these factors is responsible for the selective interaction of Aβ with DPPC domains. Interestingly, a similar preferential interaction with gel phase DPPC domains has been observed recently by AFM for both ApoE and cell-penetrating peptides [54,55]. Although both these examples led to significant peptide induced changes in membrane morphology, the overall preference for interaction with DPPC rather than surrounding fluid membrane parallels the results reported here for Aβ.

The observation that Aβ does not accumulate on the asymmetrical lower domains suggests that they contain DOPC in the upper leaflet. These asymmetric domains are not stable and slowly convert to symmetrical domains with DPPC in both leaflets. The instability of bilayers with mixtures of symmetric and asymmetric domains is analogous to previous observations for DSPC/DLPC mixtures [44]. However, there is an important difference in that the DOPC/DPPC bilayers convert to symmetric domains whereas the DLPC/DSPC bilayers undergo a rapid transleaflet lipid redistribution to give a bilayer with complete compositional asymmetry with large DSPC domains only in the top leaflet of the bilayer. Clearly additional studies are required to understand the factors that control the asymmetry and lipid mobility in bilayers with mixtures of gel and fluid phases.

Many previous studies that examined the interaction of Aβ with membranes have focused on the role of cholesterol and charged lipids or gangliosides. In most cases it was suggested that electrostatic interactions increase the local concentrations of peptide on the membrane surface, thus enhancing the aggregation efficiency. However, the present studies show that there is a strong preference for association of peptide with the ordered gel phase domains in a simple mixture of high and low

melting phosphatidylcholines. Our results indicate that charged lipids or cholesterol are not required to promote accumulation of Aβ on specific regions of the membrane. In this context, we note that our studies used 3 μM peptide which is significantly lower than the concentrations used in earlier AFM studies of Aβ [39,40]. The preferential accumulation of peptide on ordered domains in a binary lipid mixture is also of interest in the context of recent studies that implicate lipid rafts in Aβ accumulation and toxicity. For example, a number of studies in brain and cell culture show that a significant fraction of cellular Aβ is isolated from detergent resistant membrane fractions [32–34]. Other work has shown that the generation of Aβ by enzymatic cleavage of APP is regulated by partitioning into lipid rafts [37]. Of particular interest is a recent investigation reporting that the onset of memory deficit in a transgenic mouse model for Alzheimer's disease coincides with the accumulation of soluble dimeric Aβ in rafts and not with the formation of insoluble fibrils [38]. This has led to the hypothesis that Aβ aggregation may be initiated in lipid rafts with the formation of toxic oligomers at sites where they are well positioned to interfere with signal transduction. Consistent with this, an earlier study showed that small oligomers of Aβ(1–42) bind to protein-sensitive domains on B103 and hippocampal cell surfaces, and act as a potent toxin to cultured neurons [6].

Acknowledgments

Partial support from NRC's Genomics and Health Initiative (Towards Systems Biology of Brain Cell Interactions) is gratefully acknowledged. We thank Z. Lu and J. Popov for technical assistance with some experiments and Ira for assistance with TIRF microscopy.

References

[1] D.M. Walsh, I. Klyubin, J.V. Fadeeva, M.J. Rowan, D.J. Selkoe, Amyloid-β oligomers: their production, toxicity and therapeutic inhibition, Biochem. Soc. Trans. 30 (2002) 552–557.
[2] J. Kang, H.G. Lemaire, A. Unterbeck, J.M. Salbaum, C.L. Masters, K.H. Grzeschik, G. Multhaup, K. Beyreuther, B. Muller-Hill, The precursor of Alzheimer's disease amyloid A4 protein resembles a cell-surface receptor, Nature 325 (1987) 733–736.
[3] S.S. Sisodia, D.L. Price, Role of the β-amyloid protein in Alzheimer's disease, FASEB J. 9 (1995) 366–370.
[4] C.J. Pike, D. Burdick, A.J. Walencewicz, C.G. Glabe, C.W. Cotman, Neurodegeneration induced by β-amyloid peptides in vitro: the role of peptide assembly state, J. Neurosci. 13 (1993) 1676–1687.
[5] A. Lorenzo, B.A. Yankner, β-amyloid neurotoxicity requires fibril formation and is inhibited by congo red, Proc. Natl. Acad. Sci. 91 (1994) 12243–12247.
[6] M.P. Lambert, A.K. Barlow, B.A. Chromy, C. Edwards, R. Freed, M. Liosatos, T.E. Morgan, I. Rozovsky, B. Trommer, K.L. Viola, P. Wals, C. Zhang, C.E. Finch, G.A. Krafft, W.L. Klein, Diffusible, nonfibrillar ligands derived from $A\beta_{1-42}$ are potent central nervous system neurotoxins, Proc. Natl. Acad. Sci. 95 (1998) 6448–6453.
[7] R. Kayed, E. Head, J.L. Thompson, T.M. McIntire, S.C. Milton, C.W. Cotman, C.G. Glabe, Common structure of soluble amyloid oligomers implies common mechanism of pathogenesis, Science 300 (2003) 486–489.
[8] K.N. Dahlgren, A.M. Manelli, W.B. Stine Jr., L.K. Baker, G.A. Krafft, M. J. LaDu, Oligomeric and fibrillar species of amyloid-β peptides differentially affect neuronal viability, J. Biol. Chem. 277 (2002) 32046–32053.
[9] A.E. Roher, M.O. Chaney, Y.M. Kuo, S.D. Webster, W.B. Stine, L.J. Haverkamp, A.S. Woods, R.J. Cotter, J.M. Tuohy, G.A. Krafft, B.S. Bonnell, M.R. Emmerling, Morphology and toxicity of Aβ-(1–42) dimer derived from neuritic and vascular amyloid deposits of Alzheimer's disease, J. Biol. Chem. 271 (1996) 20631–20635.
[10] D.M. Hartley, D.M. Walsh, C.P. Ye, T. Diehl, S. Vasquez, P.M. Vassilev, D.B. Teplow, D.J. Selkoe, Protofibrillar intermediates of amyloid β-protein induce acute electrophysiological changes and progressive neurotoxicity in cortical neurons, J. Neurosci. 19 (1999) 8876–8884.
[11] D.M. Walsh, I. Klyubin, J.V. Fadeeva, W.K. Cullen, R. Anwyl, M.S. Wolfe, M.J. Rowan, D.J. Selkoe, Naturally secreted oligomers of amyloid β protein potently inhibit hippocampal long-term potentiation *in vivo*, Nature 416 (2002) 535–539.
[12] S. Lesne, M.T. Koh, L. Kotilinek, R. Kayed, C.G. Glabe, A. Yang, M. Gallagher, K.H. Ashe, A specific amyloid-β protein assembly in the brain impairs memory, Nature 440 (2006) 352–357.
[13] Y. Verdier, M. Zarandi, B. Penke, Amyloid β–peptide interactions with neuronal and glial cell plasma membrane: binding sites and implications for Alzheimer's disease, J. Pept. Sci. 10 (2004) 229–248.
[14] L.P. Choo-Smith, W. Garzon-Rodriguez, C.G. Glabe, W.K. Surewicz, Acceleration of amyloid fibril formation by specific binding of Aβ-(1–40) peptide to ganglioside-containing membrane vesicles, J. Biol. Chem. 272 (1997) 22987–22990.
[15] A. Kakio, S. Nishimoto, K. Yanagisawa, K. Matsuzaki, Interactions of amyloid β-protein with various gangliosides in raft-like membranes: importance of GM1 ganglioside-bound form as an endogenous seed for Alzheimer amyloid, Biochem. 41 (2002) 7385–7390.
[16] K. Yanagisawa, A. Odaka, N. Suzuki, Y. Ihara, GM1 ganglioside-bound amyloid beta-protein (Aβ): a possible form of preamyloid in Alzheimer's disease, Nat. Med. 1 (1995) 1062–1066.
[17] L.P. Choo-Smith, W.K. Surewicz, The interaction between Alzheimer amyloid β(1–40) peptide and ganglioside GM1-containing membranes, FEBS Lett. 402 (1997) 95–98.
[18] M. Bokvist, F. Lindstrom, A. Watts, G. Grobner, Two types of Alzheimer's β-amyloid (1–40) peptide membrane interactions: aggregation preventing transmembrane anchoring versus accelerated surface fibril formation, J. Mol. Biol. 335 (2004) 1039–1049.
[19] J. McLaurin, A. Chakrabartty, Membrane disruption by Alzheimer β-amyloid peptides mediated through specific binding to either phospholipids or gangliosides. Implications for neurotoxicity, J. Biol. Chem. 271 (1996) 26482–26489.
[20] C.M. Yip, J. McLaurin, Amyloid-β peptide assembly: a critical step in fibrillogenesis and membrane disruption, Biophys. J. 80 (2001) 1359–1371.
[21] J. McLaurin, T. Franklin, P.E. Fraser, A. Chakrabartty, Structural transitions associated with the interaction of Alzheimer β-amyloid peptides with gangliosides, J. Biol. Chem. 273 (1998) 4506–4515.
[22] E.E. Ambroggio, D.H. Kim, F. Separovic, C.J. Barrow, K.J. Barnham, L. A. Bagatolli, G.D. Fidelio, Surface behavior and lipid interaction of Alzheimer β-amyloid peptide 1–42: a membrane-disrupting peptide, Biophys. J. 88 (2005) 2706–2713.
[23] N. Arispe, H.B. Pollard, E. Rojas, Giant multilevel cation channels formed by Alzheimer disease amyloid beta-protein [Aβ P-(1–40)] in bilayer membranes, Proc. Natl. Acad. Sci. 90 (1993) 10573–10577.
[24] H. Lin, R. Bhatia, R. Lal, Amyloid β protein forms ion channels: implications for Alzheimer's disease pathophysiology, FASEB J. 15 (2001) 2433–2444.
[25] H. Lin, Y.J. Zhu, R. Lal, Amyloid β protein (1–40) forms calcium-permeable, Zn^{2+}-sensitive channel in reconstituted lipid vesicles, Biochem. 38 (1999) 11189–11196.
[26] S. Micelli, D. Meleleo, V. Picciarelli, E. Gallucci, Effect of sterols on β-amyloid peptide (AβP 1–40) channel formation and their properties in planar lipid membranes, Biophys. J. 86 (2004) 2231–2237.
[27] A. Quist, I. Doudevski, H. Lin, R. Azimova, D. Ng, B. Frangione, B. Kagan, J. Ghiso, R. Lal, Amyloid ion channels: a common structural link

for protein-misfolding disease, Proc. Natl. Acad. Sci. 102 (2005) 10427–10432.
[28] T. Iwatsubo, A. Odaka, N. Suzuki, H. Mizusawa, N. Nukina, Y. Ihara, Visualization of Aβ42(43) and Aβ40 in senile plaques with end-specific Aβ monoclonals: evidence that an initially deposited species is Aβ42(43), Neuron 13 (1994) 45–53.
[29] J.T. Jarrett, E.P. Berger, P.T. Lansbury Jr., The carboxy terminus of the β amyloid protein is critical for the seeding of amyloid formation: implications for the pathogenesis of Alzheimer's disease, Biochem. 32 (1993) 4693–4697.
[30] S.W. Snyder, U.S. Ladror, W.S. Wade, G.T. Wang, L.W. Barrett, E.D. Matayoshi, H.J. Huffaker, G.A. Krafft, T.F. Holzman, Amyloid-β aggregation: selective inhibition of aggregation in mixtures of amyloid with different chain lengths, Biophys. J. 67 (1994) 1216–1228.
[31] G. Bitan, M.D. Kirkitadze, A. Lomakin, S.S. Vollers, G.B. Benedek, D.B. Teplow, Amyloid β-protein (Aβ) assembly: Aβ40 and Aβ42 oligomerize through distinct pathways, Proc. Natl. Acad. Sci. 100 (2003) 330–335.
[32] S.J. Lee, U. Liyanage, P.E. Bickel, W. Xia, P.T. Lansbury, K.S. Kosik, A detergent insoluble membrane compartment contains Aβ in vivo, Nat. Med. 4 (1998) 730–734.
[33] M. Morishima, Y. Ihara, The presence of amyloid β-protein in the detergent-insoluble membrane compartment of human neuroblastoma cells, Biochem. 37 (1998) 15247–15253.
[34] S. Wahrle, P. Das, A.C. Nyborg, C. McLendon, M. Shoji, T. Kawarabayashi, L.H. Younkin, S.G. Younkin, T.E. Golde, Cholesterol-dependent γ-secretase activity in buoyant cholesterol-rich membrane microdomains, Neurobiol. Dis. 9 (2002) 11–23.
[35] K. Simons, E. Ikonen, Functional rafts in cell membranes, Nature 387 (1997) 569–572.
[36] K. Simons, D. Toomre, Lipid rafts and signal transduction, Nat. Rev., Mol. Cell Biol. 1 (2000) 31–39.
[37] R. Ehehalt, P. Keller, C. Haass, C. Thiele, K. Simons, Amyloidogenic processing of the Alzheimer β-amyloid precursor protein depends on lipid rafts, J. Cell Biol. 160 (2003) 113–123.
[38] T. Kawarabayashi, M. Shoji, L.H. Younkin, L. Wen-Lang, D.W. Dickson, T. Murakami, E. Matsubara, K. Abe, K.H. Ashe, S.G. Younkin, Dimeric Amyloid β protein rapidly accumulates in lipid rafts followed by apolipoprotein E and phosphorylated tau accumulation in the Tg2576 mouse model of Alzheimer's disease, J. Neurosci. 24 (2004) 3801–3809.
[39] J.D. Green, L. Kreplak, C. Goldsbury, X. Li Blatter, M. Stolz, G.S. Cooper, A. Seelig, J. Kistler, U. Aebi, Atomic force microscopy reveals defects within mica supported lipid bilayers induced by the amyloidogenic human amylin peptide, J. Mol. Biol. 342 (2004) 877–887.
[40] C.M. Yip, A.A. Darabie, J. McLaurin, Aβ42–peptide assembly on lipid bilayers, J. Mol. Biol. 318 (2002) 97–107.
[41] Y. Fezoui, D.M. Hartley, J.D. Harper, R. Khurana, D.M. Walsh, M.M. Condron, D.J. Selkoe, P.T. Lansbury, A.L. Fink, D.B. Teplow, An improved method of preparing the amyloid β-protein for fibrillogenesis and neurotoxicity experiments, Amyloid, Int. J. Exp. Clin. Invest. 7 (2000) 166–178.
[42] M.-C. Giocondi, V. Vie, E. Lesniewska, P.-E. Milhiet, M. Zinke-Allmang, C. Le Grimellec, Phase topology and growth of single domains in lipid bilayers, Langmuir 17 (2001) 1653–1659.
[43] H.A. Rinia, M.M.E. Snel, J.P.J.M. van der Eerden, B. de Kruijff, Visualizing detergent resistant domains in model membranes with atomic force microscopy, FEBS Lett. 501 (2001) 92–96.
[44] W.-C. Lin, C.D. Blanchette, T.V. Ratto, M.L. Longo, Lipid asymmetry in DLPC/DSPC-supported lipid bilayers: a combined AFM and fluorescence microscopy study, Biophys. J. 90 (2006) 228–237.
[45] I.A. Mastrangelo, M. Ahmed, T. Sato, W. Liu, C. Wang, P. Hough, S.O. Smith, High-resolution atomic force microscopy of soluble Aβ42 oligomers, J. Mol. Biol. 358 (2006) 106–119.
[46] W.B. Stine Jr., K.N. Dahlgren, G.A. Krafft, M.J. LaDu, In vitro characterization of conditions for amyloid-β peptide oligomerization and fibrillogenesis, J. Biol. Chem. 278 (2003) 11612–11622.
[47] S.L. Veatch, S.L. Keller, Separation of liquid phases in giant vesicles of ternary mixtures of phospholipids and cholesterol, Biophys. J. 85 (2003) 3074–3083.
[48] T.H.J. Huang, D.-S. Yang, P.E. Fraser, A. Chakrabartty, Alternate aggregation pathways of the Alzheimer β-amyloid peptide, J. Biol. Chem. 275 (2000) 36436–36440.
[49] J.J. Kremer, M.M. Pallitto, D.J. Sklansky, R.M. Murphy, Correlation of β-amyloid aggregate size and hydrophobicity with decreased bilayer fluidity of model membranes, Biochem. 39 (2000) 10309–10318.
[50] T.-L. Lau, E.E. Ambroggio, D.J. Tew, R. Cappai, C.L. Masters, G.D. Fidelio, K.J. Barnham, F. Separovic, Amyloid-β peptide disruption of lipid membranes and the effect of metal ions, J. Mol. Biol. 356 (2006) 759–770.
[51] S.A. Waschuk, E.A. Elton, A.A. Durabie, P.E. Fraser, J. McLaurin, Cellular membrane composition defines Aβ–lipid interactions, J. Biol. Chem. 276 (2001) 33561–33568.
[52] K. Florin-Casteel, G.W. Feigenson, On the use of partition coefficients to characterize the distribution of fluorescent membrane probes between coexisting gel and fluid phases: an analysis of the partition behavior of 1,6-diphenyl-1,3,5-hexatriene, Biochim. Biophys. Acta 941 (1988) 102–106.
[53] V. Koppaka, P.H. Axelsen, Accelerated accumulation of amyloid β proteins on oxidatively damaged lipid membranes, Biochem. 39 (2000) 10011–10016.
[54] K. El Kirat, L. Lins, R. Brasseur, Y.F. Dufrene, Fusogenic tilted peptides induce nanoscale holes in supported phosphatidylcholine bilayers, Langmuir 21 (2005) 3116–3121.
[55] M.E. Herbig, A. Assi, M. Textor, A.P. Merkle, The cell penetrating peptides pVEC and W2-pVEC induce transformation of gel phase domains in phospholipid bilayers without affecting their integrity, Biochem. 45 (2006) 3598–3609.